Engineering Science and Technology, an International Journal 19 (2016) 574–586

HOSTED BY

Contents lists available at ScienceDirect

Engineering Science and Technology, an International Journal

journal homepage: http://www.elsevier.com/locate/jestch

Full Length Article

Assessment of nanofluids for laminar convective heat transfer: A numerical study

Nilesh Purohit [a,*], Varun Anand Purohit [b], Kamlesh Purohit [c]

[a] BITS Pilani, Mechanical Engineering Department, Pilani, Rajasthan 333031, India
[b] AVL List GmbH Hans-List-Platz 1, Graz A-8020, Austria
[c] M.B.M, Mechanical Engineering Department, Jodhpur, Rajasthan 342001, India

ARTICLE INFO

Article history:
Received 8 July 2015
Received in revised form
13 August 2015
Accepted 14 August 2015
Available online 2 November 2015

Keywords:
Heat transfer
Laminar flow
Nanofluid
Numerical study
Comparison

ABSTRACT

In this article, a numerical study of laminar forced convective heat transfer in a circular tube is presented, incorporating entropy generation and wall shear stress analysis. Three different nanofluids, Al_2O_3–water, ZrO_2–water and TiO_2–water, are considered under constant heat flux boundary condition using single phase approach. Performance of nanofluids is compared with the base fluid by keeping the Reynolds number, mass flow rate and discharge criteria constant for various volume fractions of nanoparticles. A non linear dependence of base fluid thermo-physical properties with temperature is considered in this study. For same Reynolds number comparison criteria, the heat transfer coefficient for nanofluids is found to be significantly higher as compared to the base fluid. However, for same mass flow rate and same discharge comparison criteria, an increment in the heat transfer coefficient is found to be insignificant. The performance factor is found to be poor for the nanofluids and also, it decreases with an increase in particle loading. However, it is nearly similar for all kinds of comparisons. The entropy generation decreases for the nanofluids under same Reynolds number comparison, but the decrement is found to be negligible for the other two comparison bases. The wall shear stress increases with an increase in particle loading for all three comparisons.

1. Introduction

Colloidal suspensions made by dispersing nanoparticles (NPs) in a base fluid with various concentrations are termed as nanofluids (NFs). The concept of NFs was first materialized by Choi [1] after performing experimental investigations on various nanoparticles in Argonne National Laboratory (ANL). NPs basically are solids, which influence base fluid thermo-physical properties such as thermal conductivity, viscosity, specific heat and density [2]. The thermal conductivity of conventional base fluids increases by adding NPs, which increases heat transfer coefficient. But at the same time, viscosity also increases, which in turn increases the pumping power. The trade-off between these two contradictory effects on thermo-physical properties is vital when considering NFs as heat transfer fluids. Studies on convective heat transfer of NFs, mostly in circular tubes, could be found from the literature [3–5]. Frequently, comparing NF performance with base fluids for laminar conditions has been reported at equal Reynolds number. Li and Xuan [6] experimentally investigated Cu/water NF in a circular tube of length 800 mm and diameter 10 mm, under same Reynolds number (Re) comparison criteria and constant heat flux boundary condition. The effects of the volume fractions (0.5–2%) and the Re (800–2100) on the heat transfer and flow characteristics were examined. They declared maximum 60% enhancement in heat transfer coefficient (HTC) for 2.0% particle volume fraction. Wen and Ding [7] performed a series of experiments to investigate the effect of Re (500–2100) and particle volume fraction (0.6 and 1.6%) on the heat transfer characteristics of the y-alumina/water NF in a circular tube of length 950 mm and diameter 4.5 mm. They reported 47% enhancement in local HTC at local distance (x/D) = 63, for 1.6% particle loading (volume fraction) for Re 1600. They also utilized same Re comparison criteria under constant heat flux boundary condition. Maïga et al. [8] investigated y-alumina/water and y-alumina/ethylene glycol under constant heat flux boundary condition for Re less than 1000. They reported 67% enhancement in HTC for 7.5% particle loading (volume fraction) for Re 1000. A circular tube of length 1 m and diameter 10 mm was selected for comparing the NF performance with two different base fluids at the same Re under a wide range of

* Corresponding author. Tel.: +919950980335.
E-mail addresses: p2014010@pilani.bits-pilani.ac.in, purohitnilesh89@gmail.com (N. Purohit).
Peer review under responsibility of Karabuk University.

http://dx.doi.org/10.1016/j.jestch.2015.08.010

Table 1
Experimental studies for forced convective heat transfer of NFs for laminar flow conditions.

Author	Basis of comparison	Nanofluid	Particle loading	Reynolds no. (Re)	Geometry	Result
Li &Xuan [6]	Same Re	Cu/water	0.5–2 vol%	800–2100	D = 10 mm L = 800 mm	Heat transfer coefficient (HTC) increases up to max. 60% for 2.0 vol% particle loading.
Wen & Ding [7]	Same Re	γ-Alumina/water	0.6, 1 & 1.6 vol%	500–2100	D = 4.5 mm L = 950 mm	47% enhancement in local HTC at x/D = 63 for 1.6 vol% particle loading, Re = 1600
Maïga et al. [8]	Same Re	γ-Alumina/water, γ-Alumina/ Ethylene Glycol	0–10 vol%	250–1000	D = 10 mm L = 1m	63% enhancement in HTC for 7.5 vol% particle loading, Re = 1000
Zeinali Heris et al. [9]	Same Re	CuO/water, Alumina/water	0.2–3 vol%	650–2050	D = 6 mm L = 1m	HTC increases with decrease in particle size and increase in particle loading
Chen et al. [10]	Same Re	Titanate nanotube/water	0.5, 1.0 & 2.5 wt%	1100–2300	D = 3.9 mm L = 2m	Enhancements in local HTC at 0.5, 1.0 and 2.5 wt% at x/D = 50.4 are respectively 11.8%, 23.5% and 24.9%.
Anoop et al. [11]	Same Re	Alumina/water	1, 2, 4 & 6 wt%	500–2000	D = 4.75 mm L = 1.2m	For x/D = 147, for 45 nm particle (4 wt%) with Re = 1550, the enhancement in HTC was around 25% whereas for 150 nm particle it was found to be around 11%.
Suresh et al. [12]	Same Re	Alumina–Cu/water Hybrid	0.1 vol%	500–2000	D = 10 mm L = 1m	Max. enhancement of 13.56% in Nusselt number at a Reynolds number of 1730
Davarnejad et al. [13]	Same Re	Alumina/water	0.5–2.5 vol%	420–990	D = 6 mm L = 1m	HTC increases by increasing velocity and decreasing particle diameter
Haghighi et al. [14]	Same Re Same m* Same Q**	Alumina, Zirconia & Titanate/ water	9 wt%	200–2200	Microtube D = 0.30 mm L = 30 cm	30% enhancement in HTC when compared keeping the same Re, but negligible enhancement for other two comparison bases.
Haghighi et al. [15]	Same pumping power	Alumina, Zirconia & Titanate/ water	9 wt%	10–2300	D = 3.7 mm L = 1.5m	At equal Re comparison, HTC increased by 8–23%, whereas at equal pumping power, HTC decreased

m* = mass flow rate (kg^{s-1}), Q** = Discharge ($m^{-3}s^{-1}$), L, D = Length and diameter of test section.

particle volume fractions (0–10%). Zeinali Heris et al. [9] investigated laminar convective heat transfer of metal oxide NFs (CuO/water and alumina/water) under same Re comparison criteria for a wide range of particle loadings (0.2–3% by volume). They considered a circular tube of length 1 m and diameter 6 mm for their analysis. Also, they reported that the HTC of NFs increases with a decrease in particle size and increase in particle loading. Chen et al. [10] investigated local heat transfer characteristics of titanium oxide nanotube/water NF under laminar conditions (Re = 1100–2300) for three different particle loadings (0.5, 1 and 2.5% by weight). They utilized a circular tube of length 2 m and diameter 2.9 mm with constant heat flux boundary condition under the same Re comparison criteria for their analysis. Also, they reported enhancement in local HTC for NFs at 0.5, 1 and 2.5% particle loadings as 11.8%, 23.5% and 24.9% respectively. Similar studies [11–13] were reported showing enhancement in HTC of various NFs under laminar conditions keeping the same Re number comparison criteria.

However, a few studies were also reported with other bases of comparison. Owing to higher viscosity of NFs, they must be operated in higher mass/volume flow rates to have a Reynolds number equal to that of their corresponding base fluid. Comparing heat transfer coefficients of NFs and base fluids at equal mass flow rates, equal discharges, equal pumping powers and equal pressure drops could be a reasonable method. Haghighi et al. [14] investigated the heat transfer characteristics of three different NFs (alumina/water, zirconium oxide/water and titanium oxide/water) under laminar condition (Re = 200–2200) keeping the same Re, the same mass flow rate and the same discharge comparison criterion in a micro tube. They reported a maximum 30% enhancement in HTC when compared keeping the same Re but negligible enhancement for other two comparison bases. They also reported in another investigation for circular tube [15] that at an equal Re comparison HTC increased by 8–23% whereas at an equal pumping power comparison it decreased. The experimental studies for forced convective heat transfer of NFs for laminar flow conditions are summarized in Table 1.

Many numerical works investigating NFs are reported recently. In the year 2014, Togun et al. [16] simulated Cu/Water NF using single phase modeling approach to study its heat transfer characteristics over a backward-facing step. They reported increment in HTC for NFs over the base fluid keeping the same Re comparison criteria. In the same year, Goodarzi et al. [17] also investigated Cu/Water NF mixed convection in a rectangular shallow cavity using a two-phase mixture model. They reported that for a specific Grashof and Richardson number, the HTC increases with increase in particle loading. Safaei et al. [18] in the same year investigated multi walled carbon nanotube/Water NF in a forward facing contracting channel using single phase simulation technique. They also reported increment in HTC for NF over base fluid under the same Re criteria. No devoted numerical study, exploring comparison criteria other than same Re comparison, is found in literature. This gives the motivation to assess NFs for laminar convective heat transfer using non conventional comparison approaches.

In this study, Al_2O_3/water, ZrO_2/water and TiO_2/water NFs are numerically investigated for equal Re, equal mass flow rate and equal discharge comparison criteria under constant wall heat flux boundary condition. A complete assessment of NFs for laminar flow convective heat transfer is carried out which includes performance factor, entropy generation and wall shear stress calculations too. The particle loading is varied from 0.5% to 2% with an interval of 0.5% by volume. A circular tube with length of 1 m and diameter of 0.01 m with laminar flow conditions (Re = 1150–1900) under single phase modeling approach is adopted for the heat transfer analysis. Mass flow rates (0.006–.011 kg/s) and volume flow rates (0.08–.13 m^3/s) are selected such that the flow remains laminar under same mass flow and same volume flow rate comparison bases. Performance factor, entropy generation and average wall shear stress for all NFs are also investigated.

2. Mathematical modeling

The mathematical modeling of the NFs is done using single phase approach. In literature many studies are reported using single phase modeling to simulate NFs [19,20]. However, multi-phase techniques are more accurate and complex for simulating NFs than single

phase approach. Several recent studies are reported utilizing multi-phase modeling approaches [21–24]. For our range of investigation i.e. laminar flow, which is well defined flows, single phase modeling may be justified. Buongiorno [25] investigated seven slip mechanisms which can produce relative velocity between NP and base fluid. He reported that among investigated slip mechanisms Brownian diffusion and thermophoresis were found to be the most relevant mechanisms. Further, Ahmed et al. [26] concluded that for flows with Re higher than 100, both the Brownian force and thermophoresis may be safely neglected. This implies that homogenous behavior of the NFs is justified for our range of parameters (Re = 1150–1900). The homogenous behavior of the NF can be resolved safely using single phase modeling. Further, recently Davarnejad and Jamshidzadeh [27] investigated heat transfer performance of MgO/Water NF using single and multi-phase modeling approach and compared the simulation findings with the experimental results. They concluded that average deviation of simulation findings from experimental results for single phase approach was about 11% and that for multi-phase approach was around 2%.

2.1. Geometrical configuration

In this article, a circular tube is considered for investigating NFs as shown in Fig. 1. The ratio of L/D is so chosen to maintain a hydrodynamically developed flow at the outlet. Also, the computational domain is considered to be symmetrical with respect to the tube's main axis, so as to save computational time without compromising accuracy.

2.2. Governing equations and boundary conditions

The following governing equations are used for mathematical formulation of the single phase model [28].

Conservation of mass

$$div\left(\rho\vec{V}\right)=0 \tag{1}$$

Conservation of momentum

$$div\left(\rho\vec{V}\vec{V}\right)=-gradP+\nabla.\left(=\nabla\vec{V}\right) \tag{2}$$

Conservation of energy

$$div\left(\rho\vec{V}C_pT\right)=div\left(k\ gradT\right) \tag{3}$$

Compression work and viscous dissipation are assumed to be negligible in the energy equation. Also, source/sink term which represents integrated effects of momentum and energy exchange with base fluid is neglected. Constant velocity inlet and pressure outlet boundary conditions are applied. For heat transfer analysis, constant wall heat flux (18,000 W/m^2) boundary condition is considered.

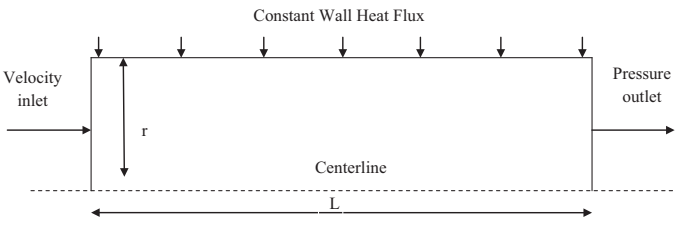

Fig. 1. Schematic of geometrical configuration under investigation.

Table 2
Thermo-physical properties of nanoparticles.

Nanoparticle	Density (kg m^{-3})	Specific heat (Jkg^{-1}K^{-1})	Thermal conductivity (Wm^{-1}K^{-1})
Alumina	3970	880	36
Zirconium oxide	5600	418	2.8
Titanium oxide	4157	710	8.4

2.3. Thermo-physical properties

In this article, the thermo-physical property of base fluid is considered temperature dependent. Also, this dependence of thermo-physical properties on temperature is non linear as shown by equations 4–7 [29,43].

$$\rho_{bf}=999.79+(0.068\times t)-(0.0107\times t^2)+(0.00082\times t^{2.5})-(2.303\times10^{-5}\times t^3)\quad \mathrm{T,t}\rightarrow\mathrm{Temperature(K,°C)} \tag{4}$$

$$k_{bf}=0.56112+(0.00193\times t)-(2.601\times10^{-6}\times t^2)-(6.08\times10^{-8}\times t^3)\quad \mathrm{T,t}\rightarrow\mathrm{Temperature(K,°C)} \tag{5}$$

$$\mu_{bf}=0.00169-(4.25\times10^{-5}\times t)+(4.92\times10^{-7}\times t^2)-(2.09\times10^{-9}\times t^3)\quad \mathrm{T,t}\rightarrow\mathrm{Temperature(K,°C)} \tag{6}$$

$$C_{bf}=4217.4-(5.61\times t)+(1.299\times t^{1.52})-(0.11\times t^2)+(4149.6\times10^{-6}\times t^{2.5})\quad \mathrm{T,t}\rightarrow\mathrm{Temperature(K,°C)} \tag{7}$$

Further, equations 8–15 are used to compute thermo-physical properties of NFs, which are assumed to be temperature independent within 300–350 K temperature range [14]. The absolute values for the thermo-physical properties for the NPs are listed in Table 2 [30].

2.3.1. Density

In this section, density of NFs is computed using Newton's mixture equation [31], which is as follows:

$$\rho_{nf}=\rho_{bf}(1-\varnothing)+\rho_p\varnothing \tag{8}$$

2.3.2. Specific Heat

The effective specific heat for all NFs is calculated using the following equation [31], which assumes thermal equilibrium between particle and the surrounding fluid:

$$c_{nf}=\frac{(1-\varnothing)(\rho c)_{bf}+\varnothing(\rho c)_p}{(\rho)_{nf}} \tag{9}$$

2.3.3. Thermal conductivity and viscosity

The thermal conductivities of the alumina and titanium oxide NFs are calculated using Maxwell model [32] i.e. equations (10) and (14). A benchmark study by Buongiorno et al. [33] justifies the use of Maxwell model for calculating the thermal conductivity of water based NFs. The equation (11) is used for calculating viscosity of alumina NF [8]. The viscosity of titanium oxide NF is calculated using equation (15), which is curve fitted and correlated by Buongiorno [34] using the results of Pak and Cho [31]. The thermal conductivity and viscosity of zirconium oxide NF are calculated using equations (12) and (13) respectively. These equations are curve fitted and correlated by Rea et al. [35], using the data of Williams et al. [36].

For Al_2O_3/Water

Table 3
Mesh independency test.

Number of grids	Average heat transfer coefficient (Wm^{-2})	Pressure drop (Pa)
15,000	632.2444	45.32
21,000	637.3937	44.17
36,000	647.1095	42.71
48,000	662.5197	40.46
60,000	683.2934	38.36
75,000	701.3921	37.12
100,000	729.7790	36.63
140,000	730.9943	36.31
220,000	732.0340	36.01
300,000	733.0980	35.81

$$K_{nf} = \frac{K_p + 2K_{bf} + 2(K_p - K_{bf})\varnothing}{K_p + 2K_{bf} - (K_p - K_{bf})\varnothing} \tag{10}$$

$$\mu_{nf} = \mu_{bf}\left(1 + 7.3\varnothing + 123\varnothing^2\right) \tag{11}$$

For ZrO2/Water

$$K_{nf} = K_{bf}\left(1 + 2.4505\varnothing - 29.867\varnothing\right) \tag{12}$$

$$\mu_{nf} = \mu_{bf}\left(1 + 46.801\varnothing + 550.82\varnothing^2\right) \tag{13}$$

For TiO2/Water

$$K_{nf} = \frac{K_p + 2K_{bf} + 2(K_p - K_{bf})\varnothing}{K_p + 2K_{bf} - (K_p - K_{bf})\varnothing} \tag{14}$$

$$\mu_{nf} = \mu_{bf}\left(1 + 5.45\varnothing + 108.2\varnothing^2\right) \tag{15}$$

2.4. Numerical method and code validation

The computational fluid dynamics code FLUENT is employed to solve the model. The governing equations (1)–(3) are solved by control volume approach. The residuals resulting from these equations are used as indicators for convergence criterion. To ensure the accuracy and the consistency of computational results, various uniform grids are tested. The result of mesh independency test shows that 100,000 numbers of grids are satisfactory to resolve local HTC and pressure drop along the pipe, as shown in Table 3. Figs. 2 and 3 also show the mesh independency test results.

In this article the heat transfer analysis is supported by three other parameters; performance factor, entropy generation and wall shear stress. Also, three different comparison approaches are used to evaluate the NFs for heat transfer fluid in laminar conditions. The local HTC is calculated using equation (16) and the average HTC is obtained by equation (17).

$$h_x = \frac{q}{(T(x)_w - T(x)_b)} \tag{16}$$

$$h_{avg} = \frac{1}{L}\int_0^L h(x)dx \tag{17}$$

By adding NPs to the base fluid, the thermal conductivity of the base fluid increases which results in increased heat transfer. Simultaneously, by adding these particles, viscosity also increases which results in increased pressure drop. Heat transfer enhancement ratio is defined as the ratio of heat transfer for NF to the heat transfer for base fluid. Similarly, pressure drop enhancement ratio is defined as the ratio of pressure drop for NF to the pressure drop for base fluid. So, to justify the use of NFs over the base fluid

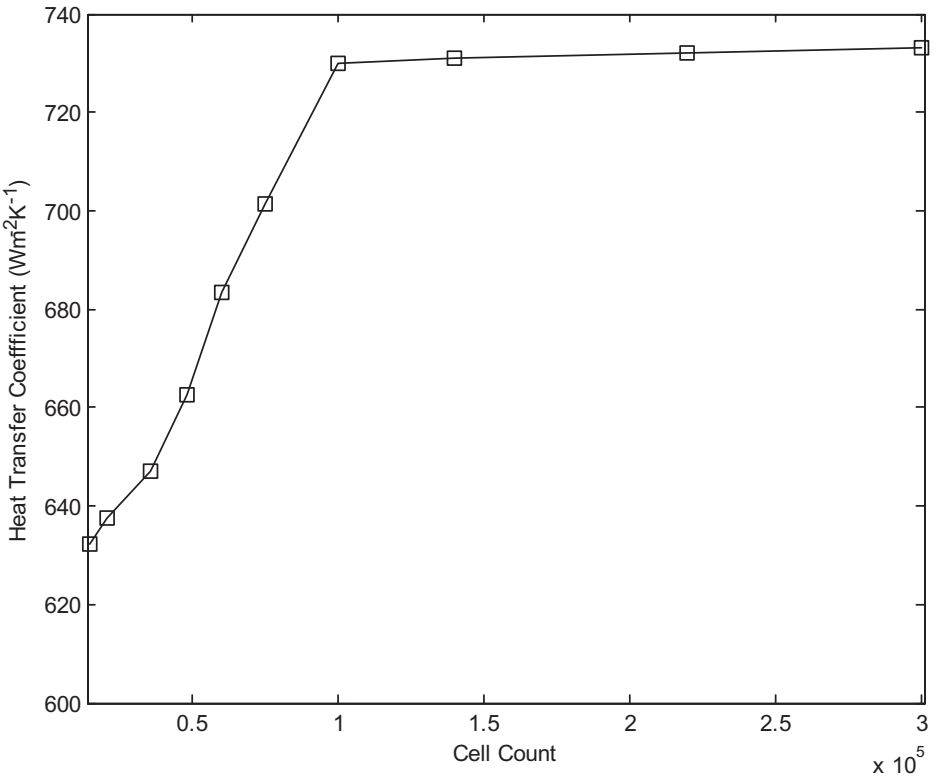

Fig. 2. Mesh independency test, local HTC vs cell count.

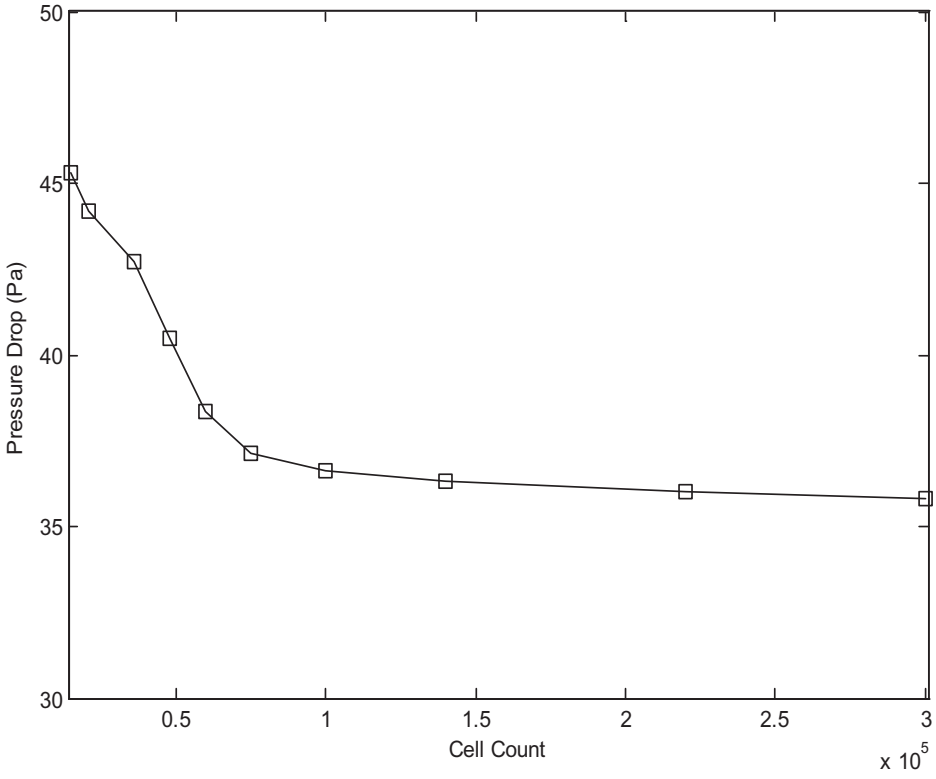

Fig. 3. Mesh independency test, pressure drop vs cell count.

or to measure the performance of NFs, thermal performance is used, which can be measured by performance factor as a function of heat transfer enhancement and pressure drop enhancement ratios. The performance factor for NFs is given as follows [37]:

$$\eta = (h_r)/(p)_r^{(1/3)} \tag{18}$$

where,

η = Performance Factor.
h_r = Heat transfer enhancement ratio.
p_r = Pressure drop enhancement ratio.

Thermodynamic second law analysis provides an additional dimension to assess NFs. Several recent studies investigating entropy generation of NFs can be found in literature [38–40]. Entropy can be defined as a measure of molecular disorder or randomness. Entropy generation as defined by the second law of thermodynamics finds its significance in measuring the complete and true performance of any thermodynamic system. Entropy generation is also a measure of entropy created by irreversibilities such as friction, heat transfer through a finite temperature difference, mixing, chemical reactions etc. In our study, fictional irreversibility and thermal irreversibility (due to heat transfer) are considered. Entropy generation is directly related to the thermodynamic efficiency and it is calculated using Bejan's equation for laminar flow [41,42] as follows:

$$S_t = S_h + S_f \tag{19}$$

$$S_h = \left((Dq^2)/(4.T_b^2.m.c.St)\right) \tag{20}$$

$$S_f = \left((2.m^3.f)/(D.A.\rho^2.T_b)\right) \tag{21}$$

where,

S_t = Total Entropy Generation (W k^{-1})
S_h = Entropy Generation Due to Heat Transfer (W k^{-1})
S_f = Entropy Generation Due to Friction (W k^{-1})

Bejan Number is defined as the ratio of entropy generation due to heat transfer to the total entropy generation. It is calculated as follows:

$$\text{Be}(\text{Bejan Number}) = (S_h/S_t) \tag{22}$$

The average wall shear stress is calculated by considering the dynamic equilibrium between the pressure drop across the cross section and the shear stress at the wall for the length of the investigated duct. For fully developed laminar flows, the fluid movement is actually not accelerating. Thus, from Newton's second law, the forces acting on the fluid must be in dynamic equilibrium. Hence, by equating pressure drop across the cross section to the shear stress across the inner surface of the tube, wall shear stress can be defined as follows:

$$\tau = \Delta p \times D/4L \tag{23}$$

$$\Delta p = \text{Pressure Drop (Pa)} \tag{24}$$

To validate the numerical results, theoretical equations are used. The correlation used for the validation of the local HTC given by Bejan [42], which is a closed form expression that covers both the entrance and the fully developed regions, is as follows:

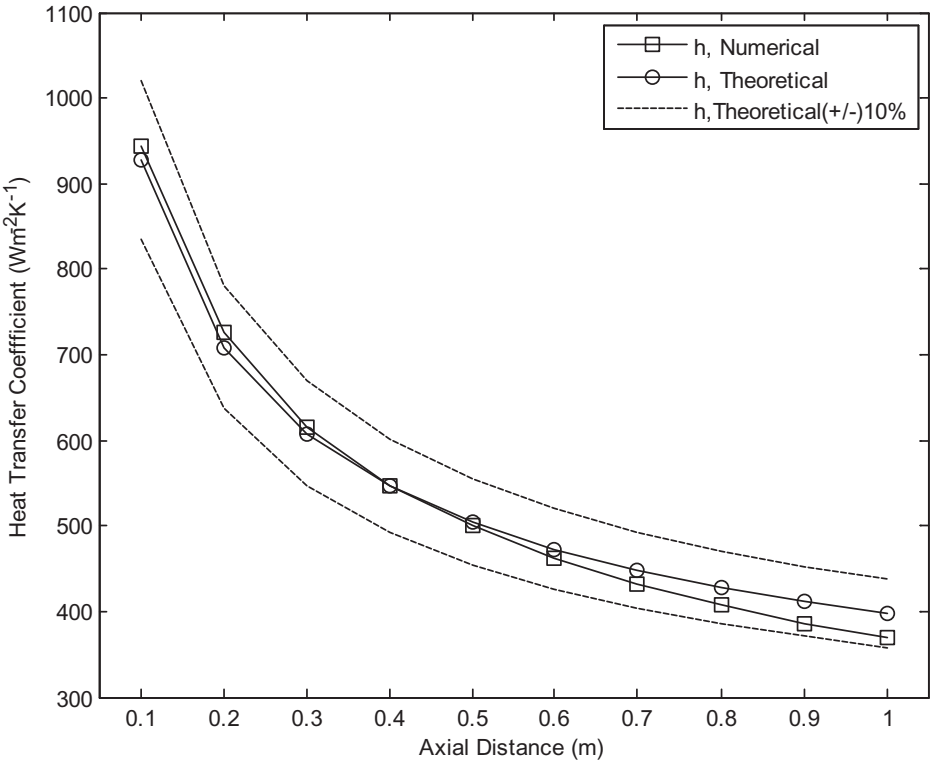

Fig. 4. Numerical values of HTC for water compared with theoretical equation.

$$\frac{Nu_x}{4.364\left(1+\left(Gz/29.6\right)^2\right)^{1/6}} = \left(1+\left(\frac{Gr/19.04}{\left(1+\left(\mathrm{Pr}/0.02\right)^{2/3}\right)^{1/2}\left(1+\left(Gz/29.6\right)^2\right)^{1/3}}\right)^{3/2}\right)^{1/3} \quad (25)$$

where,

Nu_x = Local Nusselt Number

$$Gz = \frac{\pi}{4}\times\frac{\mathrm{Re}_D\,\mathrm{Pr}}{x/D}$$

Gz = Graetz Number

Re_D = Reynolds Number based on the diameter of the pipe.

Pr = Prandtl Number

x = Axial distance (m)

D = Diameter of the pipe (m)

The pressure drop resulting from numerical solution is validated by calculating the friction factor (equation 26) and comparing the same with the standard Blasius solution [42] (equation 27) for the laminar flows. Figure 4 and Fig. 5 show the validity of results with errors less than 10%.

$$f = 2\Delta p D/(\rho L v^2) \quad (26)$$

$$f = 64/Re \quad (27)$$

3. Results and discussions

3.1. Convective heat transfer of NFs

Generally, adding NPs to the base fluid results in increment of thermal conductivity which in turn increases the heat transfer capability. Further, it increases with an increase in Re. The results for the convective heat transfer of NFs are shown in Fig. 6 and Fig. 7. For comparing all the three comparison bases a fixed particle loading of 1.5% by volume is adopted.

The main findings drawn from Fig. 6 and Fig. 7 are as follows:

- Under equal Re comparison criteria, HTC for NFs increases with increase in particle loading (0.5–2% by volume) and showed 5–18% enhancement for all investigated NFs as shown in Fig. 6.
- The trend obtained may be due to the increased mass/volume flow rates of the corresponding NFs owing to their high density and viscosity. This conventional comparison criterion is possibly misleading and not sufficient enough from a practical point of view.
- Further, the enhancement in HTC is found to be negligible, maximum up to 3%, for equal mass flow rate and equal discharge comparison bases, as shown in Fig. 7.
- For all investigated comparison criteria, alumina and zirconium NF showed superior and similar behavior while titanium oxide NF showed the minimum enhancement.

3.2. Performance factor of NFs

The performance factor of NFs depends on heat transfer and pressure drop enhancement ratios. Adding NPs to the base fluid increases

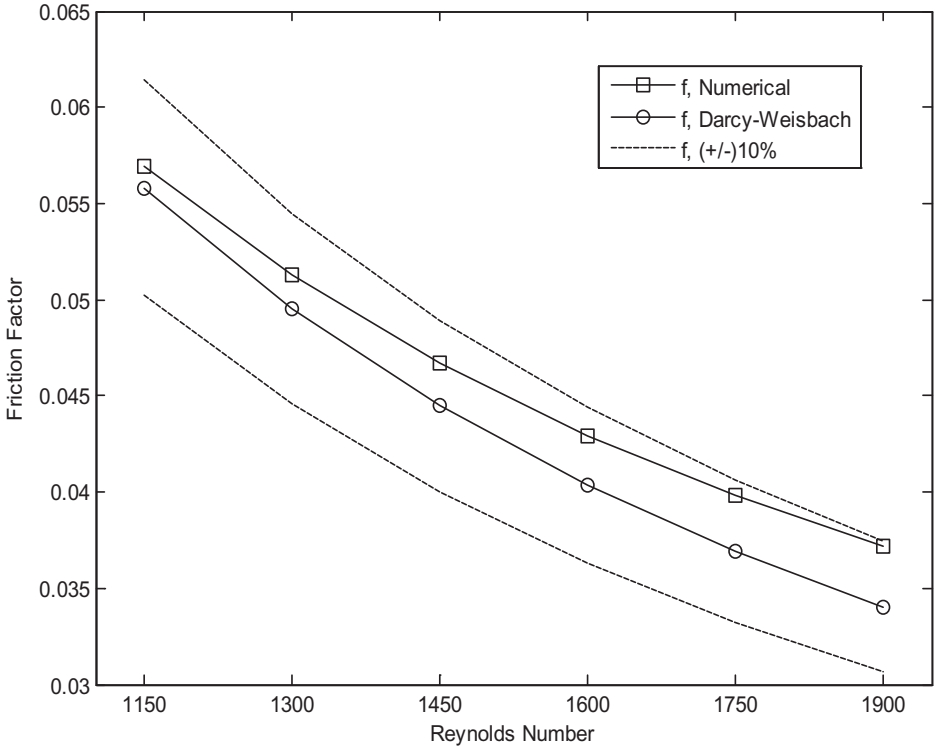

Fig. 5. Numerical values of friction factor for water compared with theoretical equation.

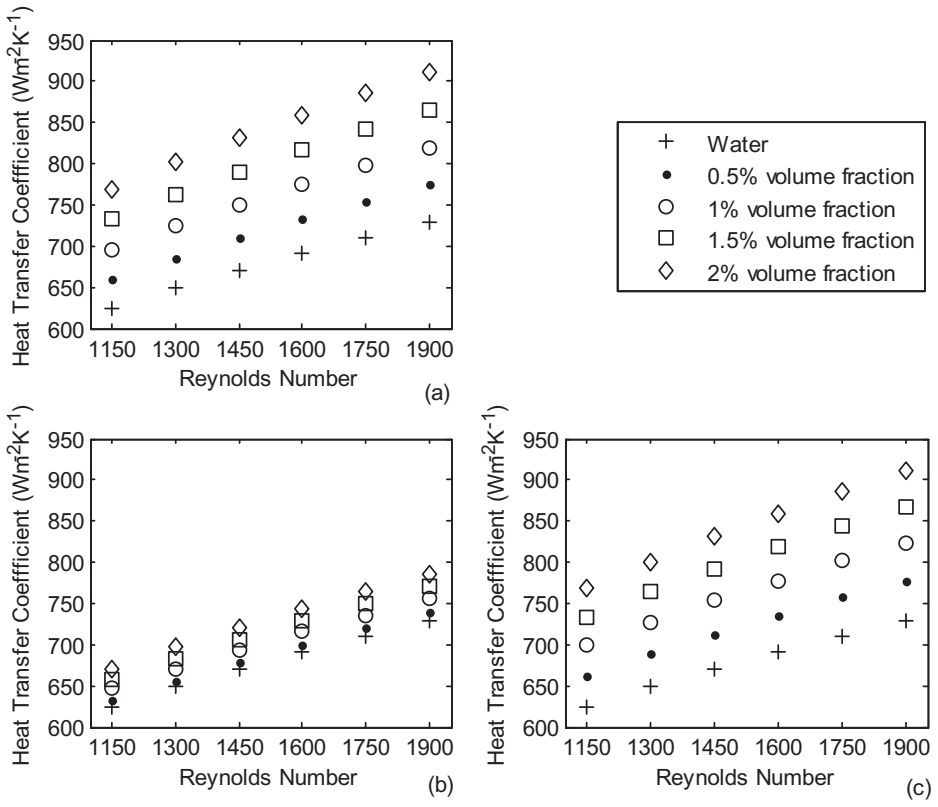

Fig. 6. Comparison of HTC for NFs with water at equal Reynolds Number for various volume fraction; (a) Alumina NF, (b) Titanium oxide NF; (c) Zirconium oxide NF.

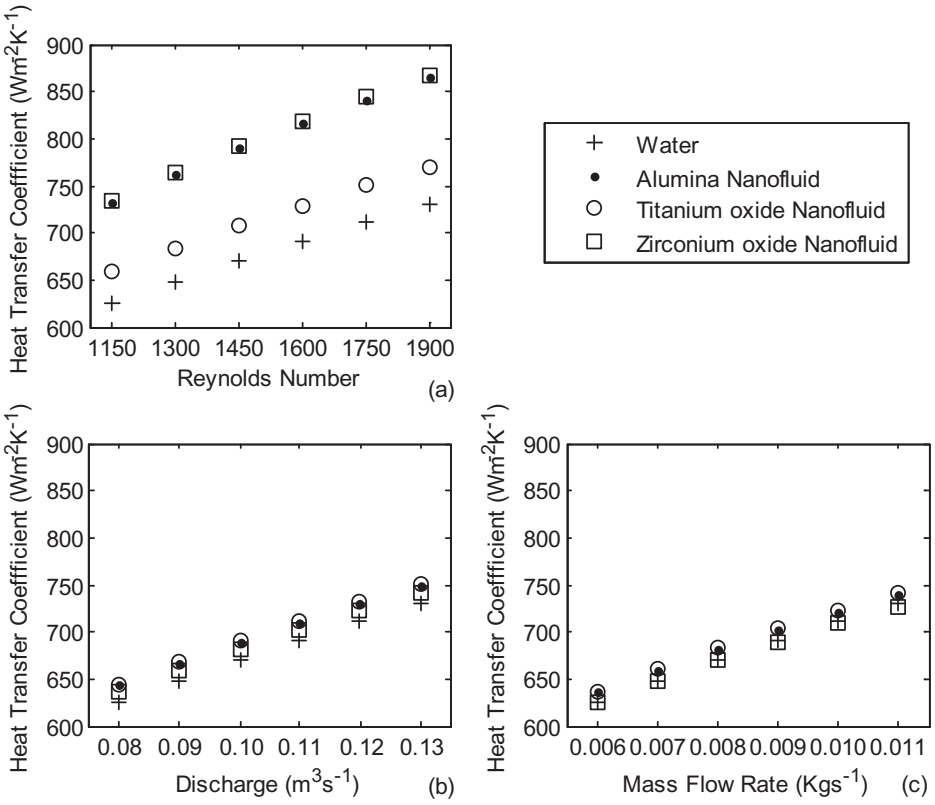

Fig. 7. Comparison of HTC for NFs with water for 1.5% volume fraction. (a) At equal Reynolds Number. (b) At equal mass flow rate. (c) At equal discharge.

the HTC due to an increase in thermal conductivity. However, NPs are heavier than base fluid; as a consequence pressure drop also increases. So, it measures the combined effect of adding NPs in the base fluid. Performance factor results for NFs are shown in Fig. 8 and Fig. 9. Generally, a performance factor above 1 is considered reasonable.

The main findings drawn from Fig. 8 and Fig. 9 are as follows:

- The performance factor was found to be poor for all NFs, regardless of the comparison criteria, as shown in Fig. 8 and Fig. 9. This may be attributed to the higher proportion increment of viscosity than HTC for NFs.
- Among all investigated cases, the maximum value for performance factor is found to be 0.9949 for titanium NF. This can be attributed to the minimum pressure drop of the titanium oxide NF due to lower viscosity rise as compared to other two NFs.
- The performance factor is found to be highest for titanium oxide NF, whereas for alumina and zirconium NFs it is found to be lower and almost similar.

3.3. Entropy generation of NFs

Entropy generation of NFs is a vital parameter that reflects the thermodynamic efficiency. The entropy generated depends on two factors namely thermal gradient and velocity gradient. The thermal gradients are responsible for the entropy generated due to the heat transfer while a velocity gradient induces entropy due to viscous effect or fluid friction. In our range of parameters (laminar flow, Re = 1150–1900) the thermal gradient factor dominates the velocity gradient indicating dominancy of heat transfer irreversibility. Further, Bejan's number is found to be nearly one in all investigated cases. Entropy generation results for NFs are shown in Fig. 10 and Fig. 11.

The main findings from Fig. 10 and Fig. 11 are as follows:

- Under equal Re comparison criteria, entropy generation for NFs decreases with increase in particle loading and showed 4.4%–14.04% decrement for all investigated NFs as shown in Fig. 10.
- However, the decrement of entropy generation is found to be negligible for the other two comparison bases, as shown in Fig. 11.
- The entropy generation decrement is found to be nearly the same for alumina and zirconium NFs, whereas for the titanium oxide NF it is found to be lower regardless of the comparison bases.

3.4. Wall shear stress of NFs

Wall shear stress is directly coupled to the pumping power as it is a function of pressure drop. Further, it is a combined function of viscosity, dimensions of the duct and the velocity, forming a non linear functionality. Since geometry is fixed, the only variables left to affect wall shear stress are viscosity and velocity. Wall shear stress results for NFs are shown in Fig. 12 and Fig. 13.

The main findings from Fig. 12 and Fig. 13 are as follows:

- Under equal Re comparison criterion, wall shear stress for NFs increases with increase in particle loading (0.5–2% by volume) and shows maximum of 3% enhancement for all investigated NFs as shown in Fig. 12.
- However, for the other two comparison bases, the increment in stress was negligible as shown in Fig. 13.
- As the particle loading increases, the non linearity in increase of wall shear stress increases due to increased viscosity of the NF at a particular Re.
- The wall shear stress is found to be highest for the zirconium NF and least for the titanium oxide NF for all type of comparison bases.

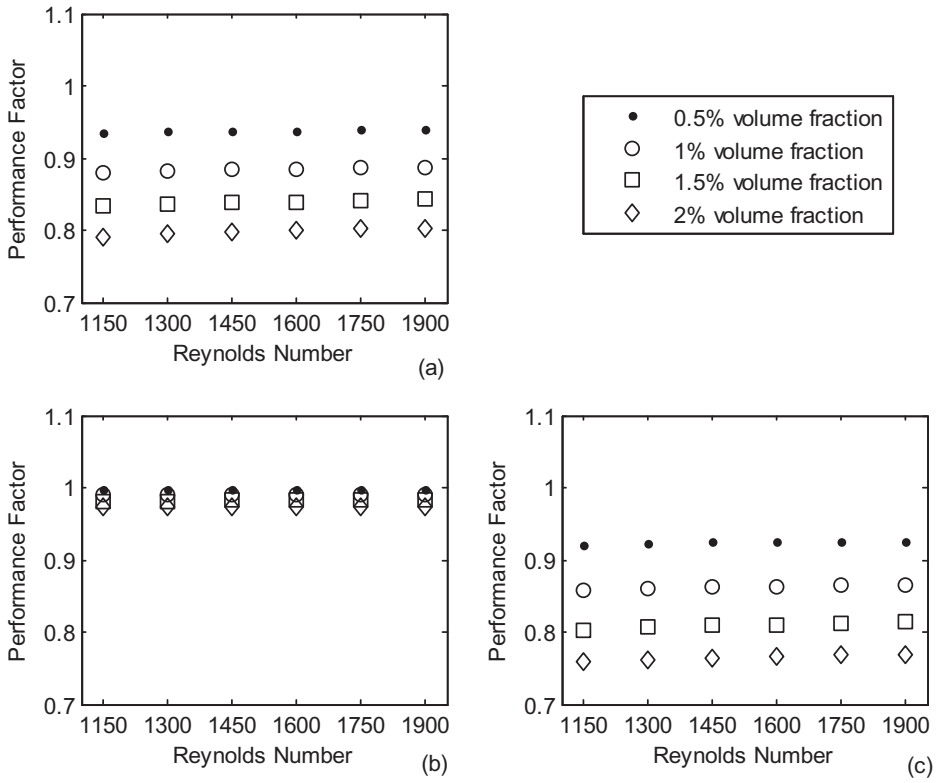

Fig. 8. Comparison of Performance for NFs with water at equal Reynolds Number for various volume fraction; (a) Alumina NF, (b) Titanium oxide NF, (c) Zirconium oxide NF.

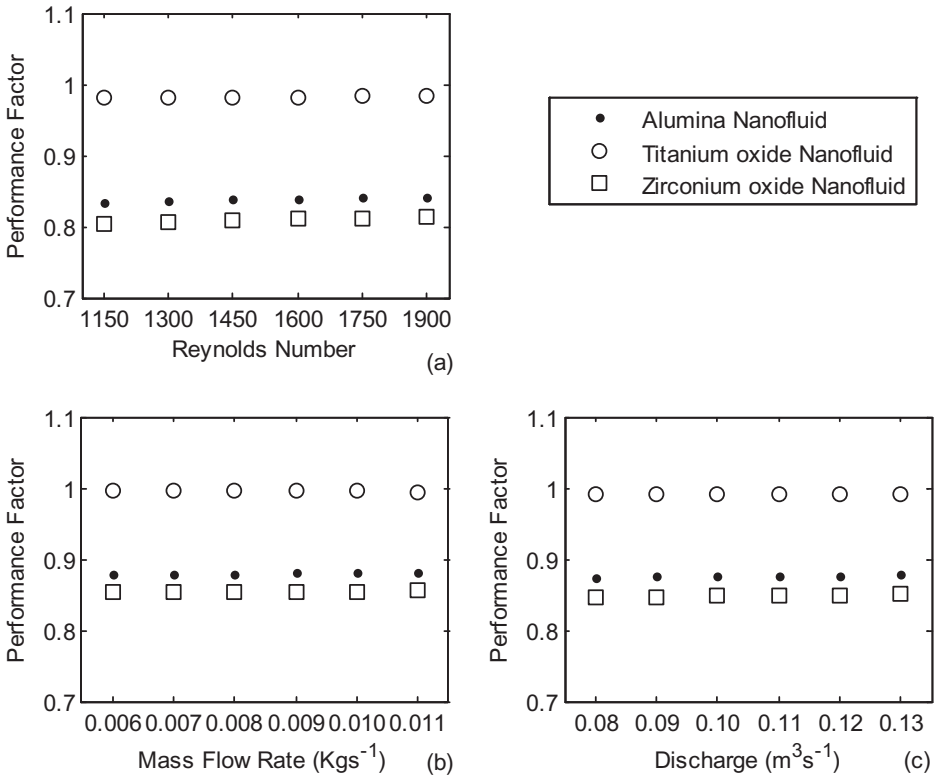

Fig. 9. Comparison of Performance Factor for NFs with water for 1.5% volume fraction. (a) At equal Reynolds Number. (b) At equal mass flow rate. (c) At equal discharge.

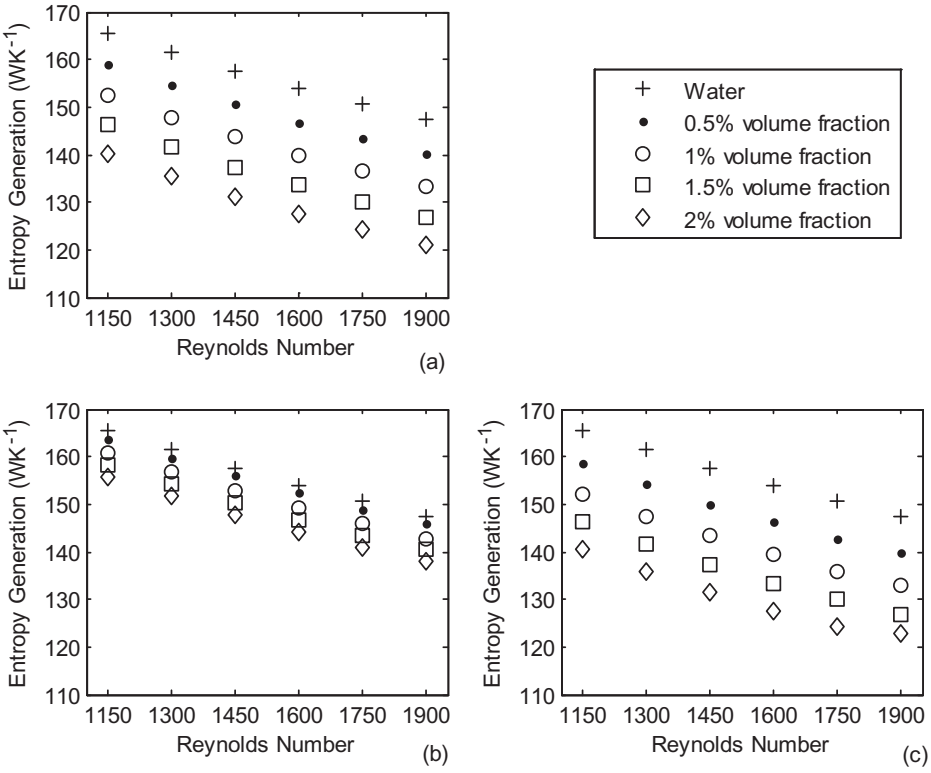

Fig. 10. Comparison of Entropy Generation for NFs with water at equal Reynolds Number for various volume fraction; (a) Alumina NF, (b) Titanium oxide NF, (c) Zirconium oxide NF.

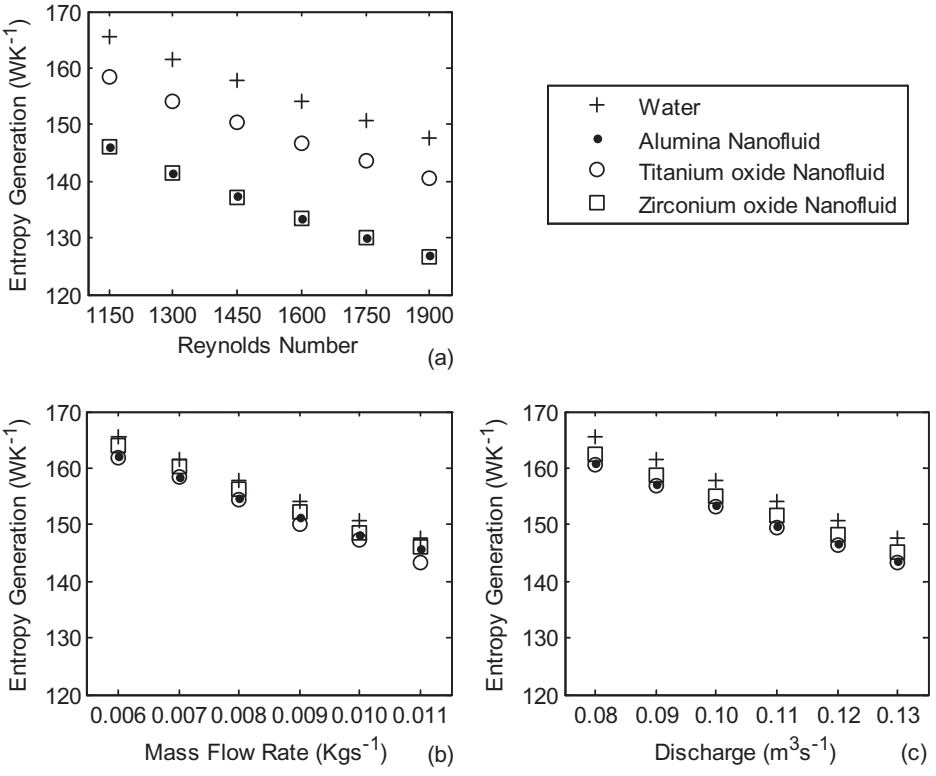

Fig. 11. Comparison of Entropy Generation for NFs with water for 1.5% volume fraction. (a) At equal Reynolds Number. (b) At equal mass flow rate. (c) At equal discharge.

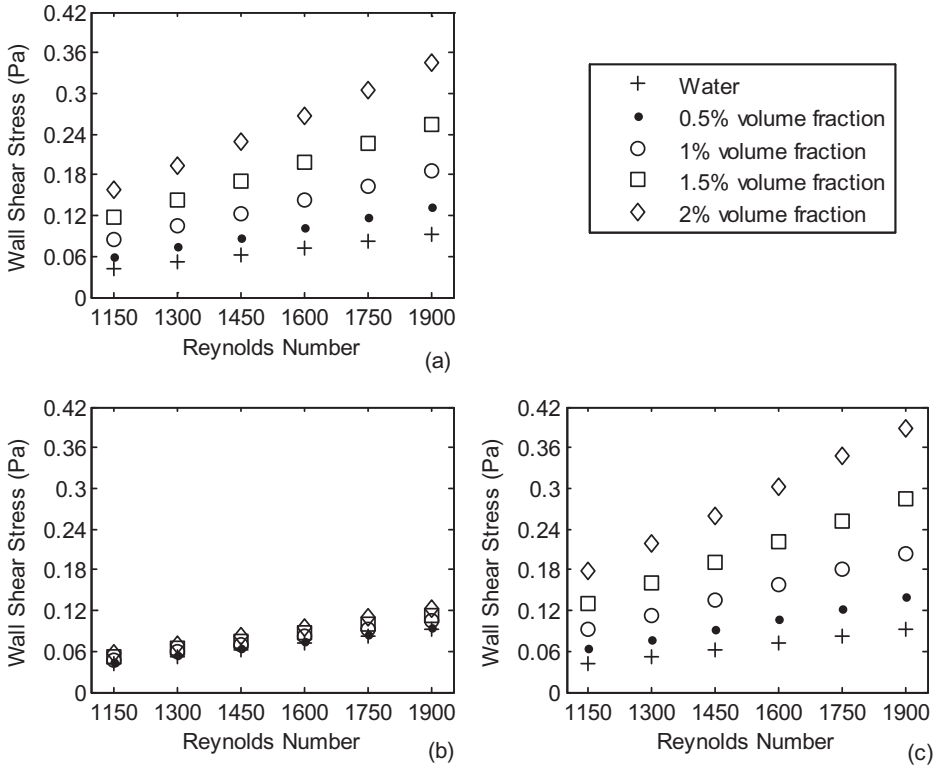

Fig. 12. Comparison of Wall Shear Stress for NFs with water at equal Reynolds Number for various volume fraction; (a) Alumina NF, (b) Titanium oxide NF, (c) Zirconium oxide NF.

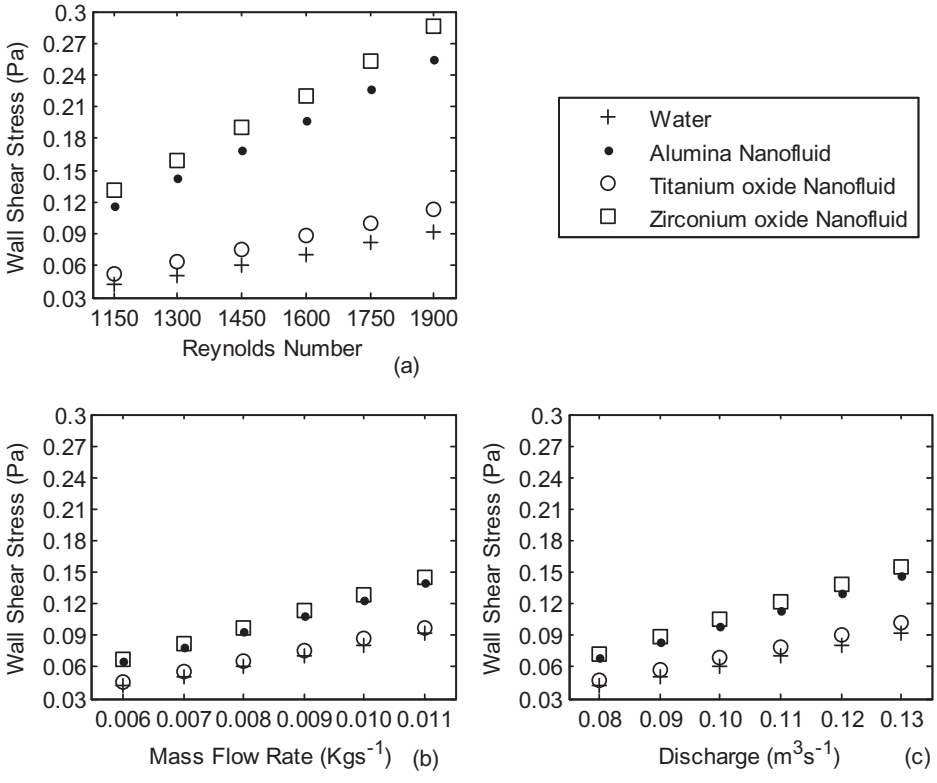

Fig. 13. Comparison of Wall Shear Stress for NFs with water for 1.5% volume fraction. (a) At equal Reynolds Number. (b) At equal mass flow rate. (c) At equal discharge.

4. Conclusions

In this article, steady state laminar convections of Al_2O_3/water, ZrO_2/water and TiO_2/water NFs were numerically investigated in a circular tube. Performance of NFs was compared with water (base fluid) using three different comparison criteria that are equal Reynolds Number, equal mass flow rate and equal discharge for both NF and base fluid. The performance of NFs depends partly on heat transfer coefficient, performance factor, entropy generation and wall shear stress, which was properly investigated here. The major conclusions drawn are as follows:

- Generally, in literature nanofluids are compared with base fluids by keeping the same Reynolds Number. However, this could be misleading. Comparing the nanofluids in such a manner resulted in a 8–30% increment of heat transfer coefficient for all investigated nanofluids. But this increment was found to be negligible for same mass flow rate and same discharge comparison bases.
- The performance factor was found to be poor for all tested nanofluids, regardless of comparison bases. Also, it was found to decrease with increase in particle loading.
- The entropy generation for nanofluids was found to decrease significantly as compared to base fluid for same Reynolds number criteria. However, this decrement was found to be negligible for the other two comparison bases. In all investigated cases, the Bejan Number was found to be nearly one, which indicates the dominance of heat transfer irreversibility.
- The wall shear stress was found to increase with increase in particle loading for all tested cases. However, the increment was found to be negligible for equal mass flow rate and equal discharge comparison bases.

In this article, no advantage was observed for employing any of the tested nanofluids over water, when the comparison is done keeping the mass flow rate and discharge the same. However, nanofluids show great potential as heat transfer fluids when the comparison basis is equal Reynolds number.

Acknowledgements

The authors would like to thank the late Dr. B.K. Maheshwari for his intense guidance and support. The authors also thank Mr. Sharad Purohit, Prof. M.S Dasgupta and Mr. Sanjeev Jakhar, for their valuable suggestions and help in this research.

Nomenclature

h	Heat Transfer Coefficient ($Wm^{-2}\,K^{-1}$)
k	Thermal Conductivity ($Wm^{-1}\,K^{-1}$)
T	Temperature (K)
C	Specific Heat ($Jkg^{-1}\,K^{-1}$)
L	Length of Tube (m)
A	Area (m^2)
D	Diameter of Tube (m)
S	Entropy Generation (WK^{-1})
m	Mass Flow Rate (kgs^{-1})
f	Friction Factor
q	Heat Flux (Wm^{-2})
St	Stanton Number
Δp	Pressure Drop (Pa)
Gz	Graetz Number
Pr	Prandtl Number
Re	Reynolds Number

Greek letters

ρ	Density (kgm^{-3})
μ	Dynamic Viscosity (Pa-sec)
∅	Particle Volume Fraction
τ	Wall Shear Stress (Pa)
η	Performance Factor

Subscripts

nf	Nanofluid
bf	Basefluid
p	Nanoparticle
x	Local Distance (m)
avg	Average
r	Ratio
w	Wall
b	Bulk
t	Total
h	Heat Transfer
f	Fluid Friction

References

[1] S. Choi, Enhancing thermal conductivity of fluids with nanoparticles, ASME-Publ.-Fed. 231 (1995) 99–106.
[2] S.K. Das, S.U. Choi, W. Yu, T. Pradee, Nanofluids: Science and Technology, John Wiley & Sons, 2007.
[3] M. Gupta, et al., A comprehensive review of experimental investigations of forced convective heat transfer characteristics for various nanofluids, Int. J. Mech. Mater. Eng. 9 (1) (2014) 1–21.
[4] A. Dalkilic, et al., Forced convective heat transfer of nanofluids – a review of the recent literature, Curr. Nanosci. 8 (6) (2012) 949–969.
[5] J. Sarkar, A critical review on convective heat transfer correlations of nanofluids, Renew. Sustain. Energy Rev. 15 (6) (2011) 3271–3277.
[6] Q. Li, Y. Xuan, Convective heat transfer and flow characteristics of Cu-water nanofluid, Sci. China Ser. E Technol. Sci. 45 (4) (2002) 408–416.
[7] D. Wen, Y. Ding, Experimental investigation into convective heat transfer of nanofluids at the entrance region under laminar flow conditions, Int. J. Heat Mass Transfe. 47 (24) (2004) 5181–5188.
[8] S.E.B. Maïga, et al., Heat transfer enhancement by using nanofluids in forced convection flows, Int. J. Heat Fluid Flow 26 (4) (2005) 530–546.
[9] S. Zeinali Heris, S.G. Etemad, M. Nasr Esfahany, Experimental investigation of oxide nanofluids laminar flow convective heat transfer, Int. Commun. Heat Mass Transfer 33 (4) (2006) 529–535.
[10] H. Chen, et al., Heat transfer and flow behaviour of aqueous suspensions of titanate nanotubes (nanofluids), Powder Technol. 183 (1) (2008) 63–72.
[11] K.B. Anoop, T. Sundararajan, S.K. Das, Effect of particle size on the convective heat transfer in nanofluid in the developing region, Int. J. Heat Mass Transfe. 52 (9–10) (2009) 2189–2195.
[12] S. Suresh, et al., Effect of Al2O3–Cu/water hybrid nanofluid in heat transfer, Exp. Therm. Fluid Sci. 38 (2012) 54–60.
[13] R. Davarnejad, S. Barati, M. Kooshki, CFD simulation of the effect of particle size on the nanofluids convective heat transfer in the developed region in a circular tube, Springer Plus 2 (1) (2013) 1–6.
[14] E.B. Haghighi, et al., Screening single phase laminar convective heat transfer of nanofluids in a micro-tube, J. Phys. Confer. Ser. 395 (2012) 012036.
[15] E.B. Haghighi, et al., Accurate basis of comparison for convective heat transfer in nanofluids, Int. Commun. Heat Mass Transfer 52 (2014) 1–7.
[16] H. Togun, et al., Numerical simulation of laminar to turbulent nanofluid flow and heat transfer over a backward-facing step, Appl. Math. Comput. 239 (2014) 153–170.
[17] M. Goodarzi, et al., Investigation of nanofluid mixed convection in a shallow cavity using a two-phase mixture model, Int. J. Therm. Sci. 75 (2014) 204–220.
[18] M.R. Safaei, et al., Investigation of heat transfer enhancement in a forward-facing contracting channel using FMWCNT nanofluids, Numer. Heat Transfer, Part A Appl. 66 (12) (2014) 1321–1340.
[19] H. Yarmand, et al., Numerical investigation of heat transfer enhancement in a rectangular heated pipe for turbulent nanofluid, Sci. World J. 2014 (2014).
[20] S. Eiamsa-ard, K. Kiatkittipong, W. Jedsadaratanachai, Heat transfer enhancement of TiO 2/water nanofluid in a heat exchanger tube equipped with overlapped dual twisted-tapes. Eng. Sci. Technol., Int. J. 18 (2015) 336–350.
[21] A. Malvandi, F. Hedayati, D. Ganji, Slip effects on unsteady stagnation point flow of a nanofluid over a stretching sheet, Powder Technol. 253 (2014) 377–384.
[22] F. Hedayati, G. Domairry, Effects of nanoparticle migration and asymmetric heating on mixed convection of TiO 2–H 2 O nanofluid inside a vertical microchannel, Powder Technol. 272 (2015) 250–259.
[23] F. Hedayati, et al., Fully developed forced convection of alumina/water nanofluid inside microchannels with asymmetric heating, Powder Technol. 269 (2015) 520–531.

[24] A. Malvandi, et al., MHD mixed convection in a vertical annulus filled with Al 2 O 3–water nanofluid considering nanoparticle migration, J. Magnet. Magn. Mater. 382 (2015) 296–306.
[25] J. Buongiorno, Convective transport in nanofluids, J. Heat Transfer 128 (3) (2006) 240–250.
[26] M. Ahmed, M. Eslamian, Laminar forced convection of a nanofluid in a microchannel: effect of flow inertia and external forces on heat transfer and fluid flow characteristics, Appl. Therm. Eng. 78 (2015) 326–338.
[27] R. Davarnejad, M. Jamshidzadeh, CFD modeling of heat transfer performance of MgO-water nanofluid under turbulent flow, Eng. Sci. Technol., Int. J. (2015). doi:10.1016/j.jestch.2015.03.011.
[28] V. Bianco, et al., Numerical investigation of nanofluids forced convection in circular tubes, Appl. Therm. Eng. 29 (17–18) (2009) 3632–3642.
[29] C. Popiel, J. Wojtkowiak, Simple formulas for thermophysical properties of liquid water for heat transfer calculations (from 0 C to 150 C), Heat Transfer Eng. 19 (3) (1998) 87–101.
[30] H. Yarmand, et al., Entropy generation during turbulent flow of zirconia-water and other nanofluids in a square cross section tube with a constant heat flux, Entropy 16 (11) (2014) 6116–6132.
[31] B.C. Pak, Y.I. Cho, Hydrodynamic and heat transfer study of dispersed fluids with submicron metallic oxide particles, Exp. Heat Transfer 11 (2) (1998) 151–170.
[32] J. Maxwell, A Treatise on Electricity End Magnetism (1873), Clarendon Press (1891), Dover, 1954.
[33] J. Buongiorno, et al., A benchmark study on the thermal conductivity of nanofluids, J. Appl. Phys. 106 (9) (2009) 094312.
[34] J. Buongiorno, Convective transport in nanofluids, J. Heat Transfer 128 (3) (2006) 240.
[35] U. Rea, et al., Laminar convective heat transfer and viscous pressure loss of alumina–water and zirconia–water nanofluids, Int. J. Heat Mass Transfe. 52 (7–8) (2009) 2042–2048.
[36] W. Williams, J. Buongiorno, L.-W. Hu, Experimental investigation of turbulent convective heat transfer and pressure loss of alumina/water and zirconia/water nanoparticle colloids (nanofluids) in horizontal tubes, J. Heat Transfer 130 (4) (2008) 042412.
[37] S. Suresh, M. Chandrasekar, S. Chandra Sekhar, Experimental studies on heat transfer and friction factor characteristics of CuO/water nanofluid under turbulent flow in a helically dimpled tube, Exp. Therm. Fluid Sci. 35 (3) (2011) 542–549.
[38] A. Malvandi, et al., An analytical study on entropy generation of nanofluids over a flat plate, Alexand. Eng. J. 52 (4) (2013) 595–604.
[39] F. Hedayati, A. Malvandi, D. Ganji, Second-law analysis of fluid flow over an isothermal moving wedge, Alexand. Eng. J. 53 (1) (2014) 1–9.
[40] M. Ghanbarpour, R. Khodabandeh, Entropy generation analysis of cylindrical heat pipe using nanofluid, Thermochim. Acta 610 (2015) 37–46.
[41] P.K. Singh, et al., Entropy generation due to flow and heat transfer in nanofluids, Int. J. Heat Mass Transfe. 53 (21–22) (2010) 4757–4767.
[42] A. Bejan, Convection Heat Transfer, John Wiley & Sons, 2013.
[43] W.H. Azmi, K.V. Sharma, R. Mamat, A.B.S. Alias, I.I. Misnon, Correlations for thermal conductivity and viscosity of water based nanofluids, in: IOP Conference Series: Materials Science and Engineering, vol. 36, IOP Publishing, 2012, p. 012029.